Selected for a Viewpoint in *Physics*
P H Y S I C A L   R E V I E W   L E T T E R S

Megavolt Parallel Potentials Arising from Double-Layer Streams in the Earth's Outer Radiation Belt

F. S. Mozer,[1] S. D. Bale,[1] J. W. Bonnell,[1] C. C. Chaston,[1] I. Roth,[1] and J. Wygant[2]

[1]*Space Sciences Laboratory, University of California, Berkeley, California 94720, USA*
[2]*Physics Department, University of Minnesota, Minneapolis, Minnesota 55455, USA*
(Received 22 August 2013; published 2 December 2013)

Huge numbers of double layers carrying electric fields parallel to the local magnetic field line have been observed on the Van Allen probes in connection with *in situ* relativistic electron acceleration in the Earth's outer radiation belt. For one case with adequate high time resolution data, 7000 double layers were observed in an interval of 1 min to produce a 230 000 V net parallel potential drop crossing the spacecraft. Lower resolution data show that this event lasted for 6 min and that more than 1 000 000 volts of net parallel potential crossed the spacecraft during this time. A double layer traverses the length of a magnetic field line in about 15 s and the orbital motion of the spacecraft perpendicular to the magnetic field was about 700 km during this 6 min interval. Thus, the instantaneous parallel potential along a single magnetic field line was the order of tens of kilovolts. Electrons on the field line might experience many such potential steps in their lifetimes to accelerate them to energies where they serve as the seed population for relativistic acceleration by coherent, large amplitude whistler mode waves. Because the double-layer speed of 3100 km/s is the order of the electron acoustic speed (and not the ion acoustic speed) of a 25 eV plasma, the double layers may result from a new electron acoustic mode. Acceleration mechanisms involving double layers may also be important in planetary radiation belts such as Jupiter, Saturn, Uranus, and Neptune, in the solar corona during flares, and in astrophysical objects.

Relativistic electrons exist in the Earth's radiation belt, other planets, the Sun, and many astrophysical objects. There is evidence that more than one acceleration mechanism is responsible for the relativistic electrons in the Earth's radiation belt. Early theoretical explanations for radiation-belt electrons involved inward radial diffusion up the night-side tail with conservation of the first two adiabatic invariants such that the perpendicular electron energy increased with the magnetic field [1]. This approach failed to explain some events in which rapid orders-of-magnitude flux increases were observed [2]. Theories of *in situ* acceleration at geocentric altitudes the order of 5 Earth radii were developed following observations that the relativistic electron phase space density was maximum at these altitudes [3]. When several hundred mV/m whistler waves were discovered in association with relativistic electron fluxes [4], the rapid acceleration was hypothesized to be due to resonant interactions of electrons with these waves. However, simulations [5,6] showed that a seed population of electrons with energies ~100 keV is required for this process to be effective. The observations, reported in this Letter, of intense trains of double layers carrying large summed potentials, might explain the origin of the required seed population.

A double layer is a region moving along the magnetic field containing charge separation such that there is an electric field and net potential step parallel to the magnetic field direction. The presence of double layers allows for the possibility that some of the electrons moving along a magnetic field line are accelerated by the sum of the potentials in a very large number of double layers. Such possibilities have been discussed in connection with auroral particle acceleration [7–11], the Earth's bow shock [12], the solar wind [13], solar flares [14–16], star formation [17], accretion into neutron stars [18], and double radio galaxies, quasars, and extragalactic jets [19,20]. Early reviews of ion acoustic double-layer theory exist in the literature [21,22].

Van Allen probes *A* and *B* were launched on August 30, 2012. During intervals discussed below, the magnetic field was within 10° of the satellite spin plane (the plane approximately normal to the Sun-Earth line) and the spin plane contained electric field measuring spheres 1, 2, 3, and 4, each at the end of a 50 meter wire [23]. Measurements were made of $(V_1\text{-}V_{sc})$, $(V_2\text{-}V_{sc})$, $(V_3\text{-}V_{sc})$, and $(V_4\text{-}V_{sc})$, where V_1 is the potential of sphere 1 and V_{sc} is the potential of the spacecraft body. These measurements were combined to give $V_{12} = [(V_1\text{-}V_{sc}) - (V_2\text{-}V_{sc})]$ as the potential difference between opposite spheres 1 and 2, as well as $V_{34} = [(V_3\text{-}V_{sc}) - (V_4\text{-}V_{sc})]$. V_{12} and V_{34} were then combined with a spin axis measurement to produce the three components of the measured electric field. This electric field data was transmitted at 512 samples/s for periods of hours and 16 384 samples/s for 5 s intervals that occurred about 1% of the time. Because resolution of the double layers requires the higher data rate, the double-layer data coverage is sparse.

During the first five months of orbital operation, the spacecraft apogee moved from near dawn to near midnight.

On 23 days during this interval, the normally positive spacecraft potential with respect to the nearby plasma was charged to negative voltages as large as -1 kV by enhanced fluxes of electrons associated with magnetic activity and relativistic electron acceleration. These spacecraft charging events lasted for many hours. On 15 of these days, sufficient high time resolution data were obtained to test whether double layers were present and double layers were found on nine of these days. The double-layer events occurred predominately near dawn and in the largest charging events. From these statistics it appears that double layers occur frequently in the 2400–0600 local time region in association with enhanced electron fluxes. The charging event on Van Allen probe B on November 1, 2012 is selected for discussion because of the fortunate circumstance of collection of 1 min of high time resolution data in a 90 s interval.

Figures 1(a)–1(c) present the full three-component measured electric field at the 16 384 samples per second time resolution in a magnetic-field-aligned coordinate system during a 160 ms interval during which the magnetic field was within 5° of the spin plane and the angle between the spin plane component of the magnetic field and the line between sphere 3, the spacecraft, and sphere 4 changed from $+2°$ to $-2°$. The electric field component perpendicular to the local magnetic field in Fig. 1(a) was composed mostly of low amplitude, few kHz, whistler mode waves while the component of 1(c), parallel to the magnetic field, showed electric field spikes which are the double layers. Each double layer contained a positive net
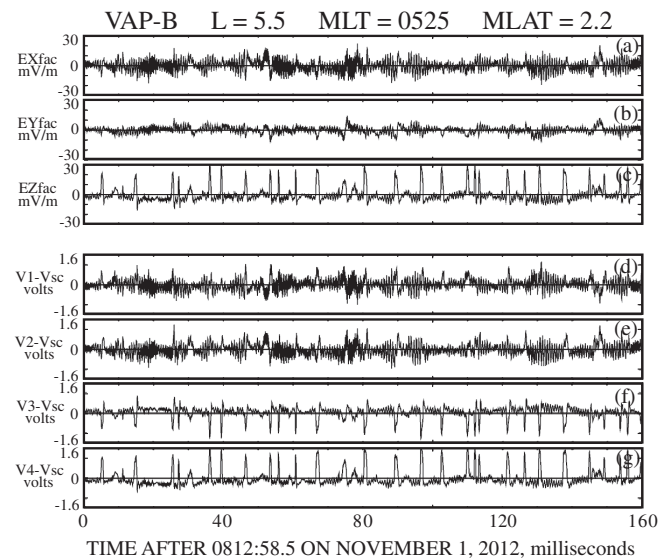
electric potential. Because these data come from an ac coupled electronics output, the resulting signal has no dc component, so the short duration positive spikes are accompanied by longer duration, lower amplitude negative signals that are an artifact of the ac coupling. The peak amplitude observed in these data is about 30 mV/m although double layers with amplitudes as great as 400 mV/m have been observed in other Van Allen probe events.

Figures 1(d)–1(g) give the four sphere potentials that exhibit low amplitude whistlers in spheres 1 and 2 and double-layer signatures in spheres 3 and 4. The fact that double-layer signatures were also seen in spheres 1 and 2 is evidence of their three-dimensional structure.

Individual sphere potentials associated with four of the double layers of Fig. 1 are illustrated in the 25 ms of data in Fig. 2(a), in which the sign of $(V_3\text{-}V_{sc})$ is inverted for easier comparison. Three estimates of the cross correlation between the sphere potentials of Fig. 1 are given in Fig. 2(b) as a function of the lag between signals $(V_4\text{-}V_{sc})$ and $(V_3\text{-}V_{sc})$. The lag is defined as the number of data points that $(V_4\text{-}V_{sc})$ led $(V_3\text{-}V_{sc})$ and is thus related to the time required for the double layers to cross the 50 m separation between sphere 4 and the spacecraft. The cross correlation obtained from the total waveform [like that in Fig. 2(a)] is the orange curve in Fig. 2(b). Because the gaps between double layers were larger than the widths of the double layers, the cross correlations might be significantly influenced by the gaps. For this reason a second cross correlation (the black curve) was obtained after setting all the negative values to zero. It is also seen in Fig. 2(a) that the double layers were perturbed during their crossing, after passing sphere 4 and before reaching sphere

VAP-B   L = 5.5   MLT = 0525   MLAT = 2.2

FIG. 1.   (a), (b), and (c) The three components of the electric field in magnetic-field-aligned coordinates in which the electric field component parallel to the magnetic field is in (c). The spiky electric field signatures containing net potentials are the double layers. (d),(e),(f), and (g) The four sphere potentials that exhibit low amplitude whistlers in spheres 1 and 2 and double-layer signatures in spheres 3 and 4.

FIG. 2 (color).   Sphere potentials for four of the double layers in Figs. 1 are given in (a) and the cross correlations between measurements made on opposite sphere pairs for all of the double layers of Fig. 1 are given in (b) for three different analyses.

3, by the large negative potential surrounding the space-craft. Thus, their fall times differed in a way that might influence the cross correlation. To eliminate this spurious effect of the double-layer perturbation by the spacecraft potential, a third cross correlation, in green, was computed from data involving only the rise times of the individual sphere voltages.

The orange cross-correlation curve for the full data set and the black curve for the data set with negative voltages set to zero both peak for a lag of about 0.1 data points. The green cross correlation for the rise time data peaks at about 0.25 data points. Thus, the average double layer crossed the 50 m separation between sphere 4 and the spacecraft in 0.2 ± 0.1 data points. At a data rate of 16 384 points/s, 0.2 points gives 12 μs. (This same delay has been determined from cross-correlation analyses of double layers on three other days.) Adding the electronic delay of 3.81 μs between sampling, the two sphere potentials give a net crossing time of 16 μs. Thus, the average double-layer speed parallel to the magnetic field was 3100 km/s, which is the electron thermal speed for a 25 eV electron. The full width at half maximum of the double layers averaged about 0.45 ms, so their widths along the magnetic field averaged about 1.4 km. The average electric field amplitude was about 20 mV/m, so the parallel potential across an average double layer was about 30 V.

To estimate the frequency, duration, and total potential of double-layer streams, a 1 min interval of parallel electric field data collected at 16 384 samples/s on the day of interest is discussed in Fig. 3. Figures 3(a) and 3(b) present 1 s examples of typical double-layer streams seen in the parallel electric field. The time of each plot is indicated in each plot and shown as the arrows in Fig. 3(c). The number of double layers in each plot is indicated in the lower left corner of each plot. [Note that the double layers of Fig. 1 occurred in Fig. 3(a).] The integral over the full minute of the electric field is shown in Fig. 3(c). The horizontal
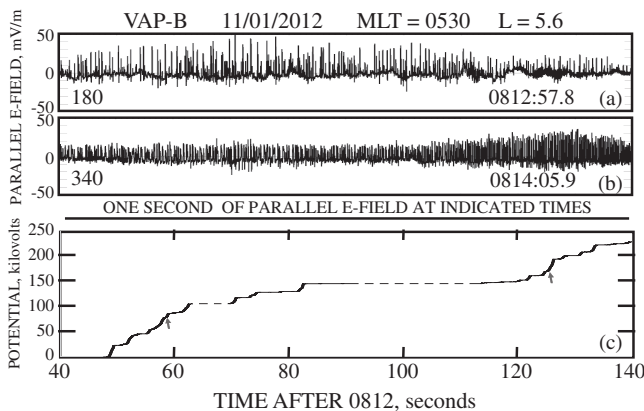
dashed lines result from the absence of high time resolution data and the horizontal solid lines covered regions where there was data and no double layers. The steps in Fig. 3(c) indicate the potential jumps associated with the few-second durations of double-layer streams that involved 7000 double layers counted during this 1 min. From Fig. 3(c), the summed potential of double layers crossing the spacecraft during this 1 min was about 230 kV. This estimate is uncertain by about 50 kV due to uncertainties in removing the low amplitude spurious signals in the data that arise from the ac coupling in the analysis electronics.

Because the data of Fig. 3 were measured during infrequent, short duration, high rate (16 384 samples/s) intervals, continuous lower rate (512 samples/s) data must be used to determine the extent in time of this event. The 0.45 ms duration double layers are undersampled at 512 Hz, so these data are subjected to further analysis in order to pull double-layer signatures out of the much larger low-frequency signals and bipolar waves (whistlers or electron holes). Figure 4 results from high-pass filtering of the 512 Hz data at 20 Hz (to remove the low frequency signals), computing the running sum of the maximum amplitude plus minimum amplitude observed in each 1 s interval (because bipolar signals sum to zero while double-layer signatures do not) and, finally, low pass filtering this running average at 0.25 Hz. Figure 4 shows that double layers occurred for about 6 min surrounding the time of Fig. 3 (the vertical dashed line) and for similar time intervals about 10 and 40 min later. Several examples of shorter duration double layers also appear at or above the noise level at times after the start of the plot such as 17, 30, 61, 65, 70, and 84 min. Because the 1 min duration, 230 kV events of Fig. 3 actually lasted 6 min, more than 1 000 000 volts of electric potential is estimated to have crossed the spacecraft in this 6 min. During this time, the orbital motion of the spacecraft was about 700 km perpendicular to the magnetic field.

The double layers were observed at different times and on different magnetic field lines, so the instantaneous parallel potential along a single field line has to be estimated from these large double-layer events. At the speed of

FIG. 3. (a),(b) 1 s examples of double layers observed during 1 min of high time-resolution data. (c) The integrated electric potential over the 1 min of data. The steps in (c) indicate the potential jumps associated with individual double-layer streams.
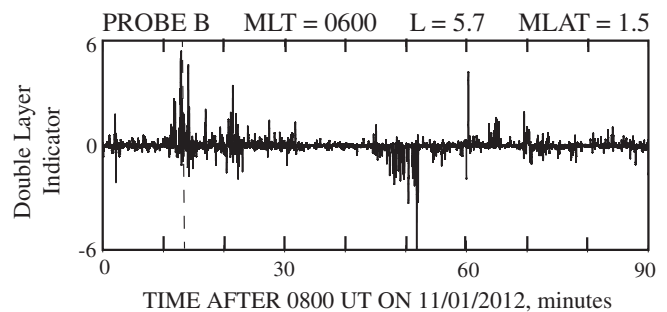
FIG. 4. The double-layer indicator that shows when double-layer events occurred during the 90 min around the event of interest.

3100 km/s, a double layer traverses the length of the magnetic field line in about 15 s. Thus, the instantaneous potential along a field line was the order of the individual steps in Fig. 3(c), or tens of kilovolts. Following such a step, one or more successive voltage steps might occur on the same field line or on a nearby neighbor. Thus, the total potential experienced by a charged particle might be a multiple of this instantaneous potential drop.

This large potential is produced in a self-consistent interaction with the electron plasma and it could result in acceleration or even suppression of electron transport [24]. The seed electrons required for efficient resonant acceleration by coherent whistler waves [5,6] might be produced by double layers. Perhaps, x-ray microbursts seen on balloons [25] result from electrons accelerated by double layers. At any rate, the observed double layers must play a significant role in radiation belt dynamics.

The observed double layers travel at the 25 eV electron thermal or acoustic speed. This differs from the speed of an ion acoustic double layer composed of single temperature ions and single temperature electrons in which the double layers travel roughly at the ion acoustic speed. This discrepancy gives rise to the possibility of a new double-layer model stemming from a multitemperature electron distribution with the low energy electrons playing the role of the ions in the ion acoustic theory. Some properties of the electron acoustic mode have been discussed [26–28] in which it has been concluded that the mode may be excited when the hot-to-cold electron temperature ratio becomes sufficiently large (~ 10) while the cold-to-hot density ratio is sufficiently small (~ 0.1). In these circumstances, the role of the ions in the ion acoustic mode is replaced by the cold electron population, resulting in a much higher phase velocity. As the wave grows and saturates, it traps electrons, forming an additional non-Maxwellian component. When the electric potential is much larger than the cold electron temperature, the wave reaches a strongly nonlinear regime involving significant deformation of the electron trajectories.

The possible association of double layers with relativistic electron acceleration is illustrated in Fig. 5 which gives five days of electric field, magnetic field [29], and energetic electron data [30] from the Van Allen probes. Figure 5(a) gives the flux of 2.5 MeV electrons [31] which shows a nearly 3 orders-of-magnitude increase in a fraction of a day. The electric field data in panels 5(b), 5(d), and 5(e) were obtained from 5 s bursts at a sample rate of 16 384 Hz. These bursts occurred about 1% of the total time interval in the figure. Figure 5(b) gives this burst rate in events/h and also shows, in red, the 9 times during which intense streams of double layers were observed. Double layers could have existed at later times than those shown on October 9, 2012, but such data are not available due to detector saturation associated with spacecraft charging in the enhanced electron fluxes. Figure 5(c) plots a
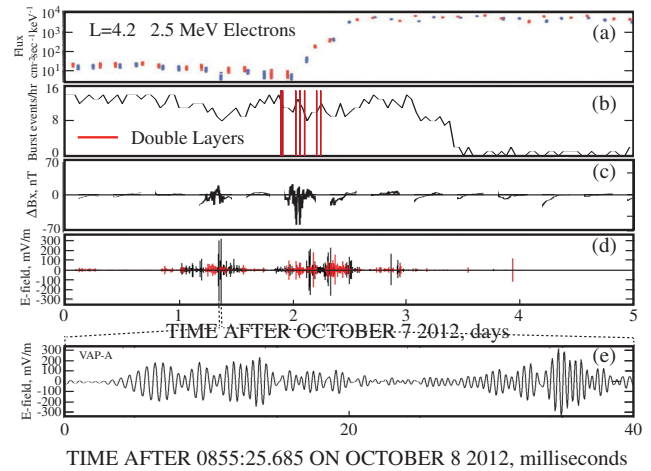
FIG. 5 (color). (a) Five days of data during which electrons were accelerated to relativistic energies. (b) The nine times that double layers were observed, in red. (c) Perpendicular component of the magnetic field that is associated with field-aligned currents. (d) Whistler waves observed in the 1% of data collected at high time resolution. (e) Expanded view of one whistler wave packet, showing electric fields as large as 300 mV/m.

perpendicular component of the difference between the measured magnetic field and a model field in the model field frame of reference, in which data near perigees has been deleted. This plot gives a magnetic field component associated with a field-aligned current. At the time of the flux increase, and to a lesser extent the previous day, there is a signature of a field-aligned current that suggests the observed double layers are of the current driven type. Figure 5(d) gives waveform data showing that large amplitude whistlers (~ 300 mV/m) were observed in the 1% of data caught by the burst detector. They occurred on the day of electron acceleration, October 9, as well as during the previous day. Panel 5(e) expands the largest observed whistlers in a 40 ms duration plot.

Figure 5 illustrates two candidate acceleration events, one on October 8 and the other on October 9. The October 8 event occurred during a southward interplanetary magnetic field (not shown) and had a field-aligned current and large amplitude whistler waves. It had no double layers and the MeV plasma was not enhanced. The event on October 9 also occurred during a southward interplanetary magnetic field, a field-aligned current and large amplitude whistlers, but it also had double layers and significant relativistic electron acceleration. This suggests that the double layers may be a necessary ingredient for relativistic electron acceleration, possibly because they make the required seed population. Indeed, the flux of 100 keV electrons on October 9 was larger than that on October 8, which supports this view.

Theories of particle acceleration in solar flares [14–16], star formation [17], accretion into neutron stars [18], and double radio galaxies, quasars, and extragalactic jets [19,20] have also invoked double layers. So these

observations in the terrestrial magnetosphere may be important in other planetary radiation belts such as Jupiter, Saturn, Uranus, and Neptune [32], in the solar corona during flares, and in astrophysical objects.

[1] M. Shulz and L. J. Lanzerotti, *Physics and Chemistry in Space* (Springer, New York, 1975), Vol. 7.

[2] X. Li, D. N. Baker, M. Teremin, T. E. Cayton, G. D. Reeves, R. S. Selesnick, J. B. Blake, G. Lu, S. G. Kanekal, and H. J. Singer, J. Geophys. Res. **104**, 4467 (1999).

[3] R. S. Selesnick and J. B. Blake, J. Geophys. Res. **105**, 2607 (2000).

[4] C. Cattell *et al.*, Geophys. Res. Lett. **35**, L01105 (2008).

[5] I. Roth, M. Temerin, and M. K. Hudson, Ann. Geophys. **17**, 631 (1999).

[6] Y. Omura, N. Furuya, and D. Summers, J. Geophys. Res. **112**, A06236 (2007).

[7] H. Alfvén, Tellus **10**, 104 (1958).

[8] L. P. Block, Astrophys. Space Sci. **55**, 59 (1978).

[9] F. S. Mozer, C. W. Carlson, M. K. Hudson, R. B. Torbert, B. Parady, J. Yatteau, and M. C. Kelley, Phys. Rev. Lett. **38**, 292 (1977).

[10] R. E. Ergun, L. Andersson, D. S. Main, Y.-J. Su, C. W. Carlson, J. P. McFadden, and F. S. Mozer, Phys. Plasmas **9**, 3685 (2002).

[11] M. Temerin, K. Cerny, W. Lotko, and F. S. Mozer, Phys. Rev. Lett. **48**, 1175 (1982).

[12] S. D. Bale and F. S. Mozer, Phys. Rev. Lett. **98**, 205001 (2007).

[13] A. Mangeney, C. Salem, C. Lacombe, J.-L. Bougeret, C. Perche, R. Manning, P. J. Kellogg, K. Goetz, S. J. Monson, and J.-M. Bosqued, Ann. Geophys. **17**, 307 (1999).

[14] C. Jacobsen and P. Carlquist, Icarus **3**, 270 (1964).

[15] H. Alfvén and P. Carlquist, Sol. Phys. **1**, 220 (1967).

[16] S. S. Hasan and D. Ter Haar, Astrophys. Space Sci. **56**, 89 (1978).

[17] H. Alfven and P. Carlqvist, Astrophys. Space Sci. **55**, 487 (1978).

[18] A. C. Williams, M. C. Weisskopf, R. F. Elsner, W. Darbro, and P. G. Sutherland, Astrophys. J. **305**, 759 (1986).

[19] A. L. Peratt, IEEE Trans. Plasma Sci. **14**, 639 (1986).

[20] J. Borovsky, Laser Part. Beams **5**, 169 (1987).

[21] H. Schamel, Phys. Rep. **140**, 161 (1986).

[22] M. A. Raadu and J. J. Rasmussen, Astrophys. Space Sci. **144**, 43 (1988), http://link.springer.com/article/10.1007/BF00793172.

[23] J. R. Wygant *et al.*, Space Sci. Rev. **179**, 183 (2013).

[24] T. C. Li, J. F. Drake, and M. Swisdak, Astrophys. J. **757**, 20 (2012).

[25] K. A. Anderson and D. W. Milton, J. Geophys. Res. **69**, 4457 (1964).

[26] I. Roth and M. K. Hudson, J. Geophys. Res. **91**, 8001 (1986).

[27] S. P. Gary and R. L. Tokar, Phys. Fluids **28**, 2439 (1985).

[28] R. Pottelette, R. E. Ergun, R. A. Treumann, M. Berthomier, C. W. Carlson, J. P. McFadden, and I. Roth, Geophys. Res. Lett. **26**, 2629 (1999).

[29] C. A. Kletzing *et al.*, Space Sci. Rev. **179**, 127 (2013).

[30] H. E. Spence *et al.*, Space Sci. Rev. **179**, 311 (2013).

[31] G. D. Reeves *et al.*, Science **341**, 991 (2013).

[32] B. H. Mauk and N. J. Fox, J. Geophys. Res. **115**, A12 220 (2010).